Liquid Taylor Bubbles Rising in a Vertical Column of a Heavier Liquid: An Approximate Analysis

T. K. Mandal
Department of Chemical Engineering,
National Institute of Technology,
Durgapur WB-713209, India
e-mail: tapasmn@gmail.com

G. Das[1]
Department of Chemical Engineering,
Indian Institute of Technology,
Kharagpur WB-721302, India
e-mail: gargi@che.iitkgp.ernet.in

P. K. Das
Department of Mechanical Engineering,
Indian Institute of Technology,
Kharagpur WB-721302, India
e-mail: pkd@mech.iitkgp.ernet.in

It has been noted that a volume of lighter liquid when injected into a stationary column of a heavier liquid, it rises up as a simple elongated Taylor bubble. In the present study, experimental and theoretical analyses have been performed to understand the rise of liquid Taylor bubbles. The experiments have been performed with different liquid pairs with their viscosities ranging from 0.71 mPa s to 1.75 mPa s and conduit sizes ranging from 0.012 m to 0.0461 m. The bubble shape has been predicted using a potential flow analysis and validated from photographic measurements. This analysis has been further modified to predict the rise velocity. The modified analysis accounts for the density difference between the two liquids, viscosity effects of the primary liquid, and interfacial tension of two fluids. A semi-empirical equation has been developed, which gives satisfactory results for most of the cases. [DOI: 10.1115/1.3026730]

Keywords: liquid Taylor bubble, shape, rise velocity, mathematical modeling, viscous potential flow

1 Introduction

Taylor bubbles (TBs) are typical elongated gas bubbles, which occupy almost the entire cross section of a liquid filled conduit and move along its axis. In a circular tube they are characterized by an axisymmetric bullet shaped nose, a cylindrical body, and a flat or jagged tail (Fig. 1). However, the shape of the Taylor bubble depends to a larger extent on the cross section [1–3] and inclination of the conduit and to a smaller extent on the properties of the fluid pair. The shape is also sensitive to the size of the conduit. For example, Taylor bubbles observed in narrow circular tubes have a dome shaped nose and tail [4,5], while in a wider conduit, these are characterized by a hemispherical nose and a flat tail. Taylor bubbles are observed in a myriad of gas-liquid two-phase systems. During the drainage of the liquid from a liquid filled vertical tube whose top end is closed, the rising gas finger assumes the characteristic shape of a Taylor bubble. In slug flow, Taylor bubbles and liquid slugs follow one another in rapid succession.

Over the years, the hydrodynamics of Taylor bubbles have attracted the attention of a number of researchers. In their pioneering works Dumitrescu [6] and Davies and Taylor [7] theoretically analyzed the motion of elongated gas bubbles rising through a vertical tube filled with an ideal fluid. Later the same problem was investigated comprehensively using theoretical [8–13], experimental [1,14–20], and numerical [21–25] techniques. In addition, studies have been performed to investigate the effect of liquid properties such as surface tension [26–30] and viscosity [31–36], liquid velocity, conduit geometry [4,37,38], and inclination [1,15,16] on the dynamics of Taylor bubbles. Nevertheless, the complexity of the problem could not be resolved completely as one can appreciate from the large number of correlations proposed in literature [39–41]. Recently Viana et al. [42] considered a voluminous data bank of experimental results and proposed a universal correlation for the rise velocity of Taylor bubbles through circular tubes.

When a lighter liquid is introduced in a tube filled with another immiscible and heavier liquid, it rises up as a single elongated drop, which is similar in shape to that of a Taylor bubble, as shown in Fig. 1. The dynamics of such liquid Taylor bubbles (LTBs) play an important role in the transport of liquid-liquid two-phase mixtures through conduits. However, the motion of a LTB has rarely been investigated except for a few brief mentions [1]. Brauner and Ullmann [43,44] studied gas entrainment from a Taylor bubble for moving and stationary bubbles. In the present work the motion of LTB through vertical tubes has been studied experimentally for different liquid-liquid systems and tube diameters. The theoretical models available in literature for gas-liquid systems have been modified to predict the shape and rise velocity of the LTBs. No such study has to date been reported on the rise of a liquid Taylor bubble to the best of the author's knowledge.

2 Experiments

The schematic of the experimental facility is shown in Fig. 2. The main component of the setup is a 1.5 m long borosilicate glass tube G pivoted to a frame F to facilitate free rotation. The tube is closed at both ends. Near the ends two small side tubes N_1 and N_2 are provided with valve connections. They are used for filling up and emptying the tube with the test liquids. Experiments have been conducted in tubes of different internal diameters ranging from 0.012 m to 0.0461 m. The liquids used and their measured properties are listed in Table 1. The viscosity, surface tension, and specific gravity of the individual liquids are measured using an Ostwald viscometer, stalagmometer, and electronic balance, respectively, while the interfacial tension between different liquid pairs is estimated using a ring tensiometer. The liquid properties are measured several times and the average values are taken to minimize experimental errors.

As the hydrodynamics of the bubble is sensitive to any trace of impurity, the tubes are thoroughly cleaned before using a particular pair of liquids. They are washed with detergent solution and distilled water to remove any dirt or grease. Then they are rinsed with acetone and dried. The tube is first completely filled up with the heavier liquid (henceforth referred to as the primary liquid). The lighter liquid designated as the secondary liquid is slowly introduced through the side tube N_1 keeping G in the vertical position. During this process, an identical volume of primary liq-

[1]Corresponding author.

Contributed by the Fluids Engineering Division of ASME for publication in the JOURNAL OF FLUIDS ENGINEERING. Manuscript received December 9, 2007; final manuscript received September 3, 2008; published online December 2, 2008. Assoc. Editor: Theodore Heindel.

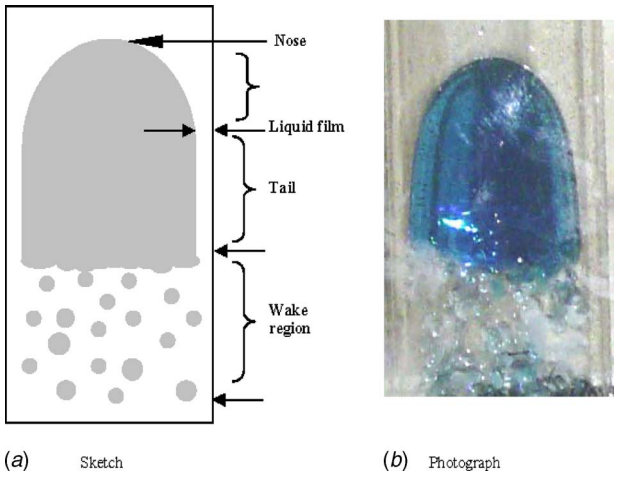

Fig. 1 Kerosene Taylor bubble rising in water: (*a*) sketch and (*b*) photograph

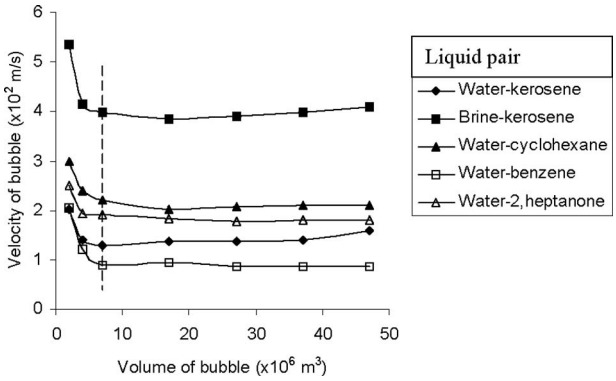

Fig. 3 Experimental values of the bubble velocity as a function of the bubble volume for the different pairs of liquids studied

uid is discharged through tube N_2. Both valves are closed once a required amount of secondary liquid is introduced into the tube. Extreme care is taken to ensure that no air bubble gets entrapped inside the tube during the process of filling up since visual observations reveal that the small air bubbles get attached to the tip of the LTB. This renders the tip pointed and increases the rise velocity substantially.

For studying the rise of LTB, the tube is inverted so that the secondary liquid occupies the bottommost position. The secondary fluid assumes the typical shape of a Taylor bubble and rises by downward displacement of the heaver fluid. Its rise velocity is estimated by noting the time of travel between two markings (P_1 and P_2) at a known distance (0.5 m apart). The markings are made at a distance 0.5 m from each end of the tube. These markings are made away from the entry and exit of the tube to avoid end effects, if any. In order to ensure that the LTB acquires its terminal rise velocity before reaching the first marking, several velocity measurements have been made over different length intervals at various positions of the tube. It is noted that the velocity thus obtained remains constant over different distances after about 0.45 m from the entry section. Therefore a distance of 0.5 m has been selected from the entry and exit sections for the experiments, and the velocity has been measured from the time taken by the LTB to traverse a distance of 0.5 m. A number of typical bubbles are photographed using a digital camera (Sony, DSC F717), near the marking P_2. During photography we used a rectangular glass view box (VB) (in Fig. 2) to minimize the effects of reflection and refraction at the curved tube surface. The rise velocities for a given volume of LTB are measured at least five times and the average value is registered. The velocity has also been measured using the optical probe technique described by Jana et al. [45] as an additional check. The uncertainties in measurements have been obtained as $\pm 0.5\%$.

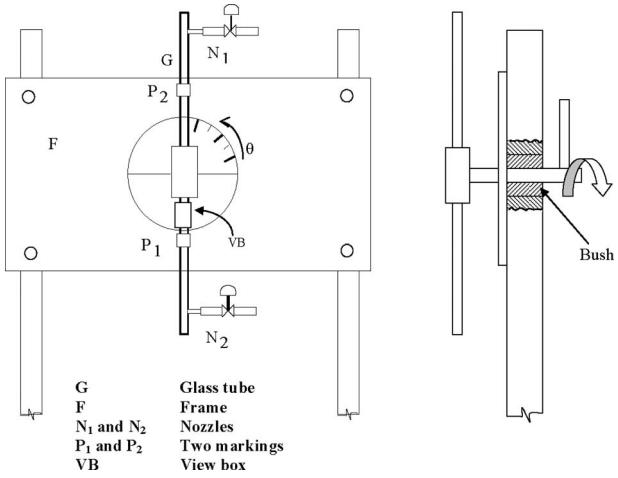

Fig. 2 Schematic of the experimental facility

Table 1 Physical properties of test liquids

Fluid	Density (kg/m^3)	Viscosity (mPa s)	Interfacial tension with water (N/m)
Water	1000	1	—
Kerosene	787	1.2	0.0385
Benzene	879	0.73	0.0356
Cyclohexane	775	0.96	0.0585
2,heptanone	810	0.71	0.0208
Brine solution	1200	1.75	0.0378 (With kerosene)

3 Results and Discussions

A typical curve representing the variation of rise velocity with bubble volume has been plotted in Fig. 3. The figure shows that rise velocity decreases sharply with an increase in bubble volume for all the cases and finally attains an asymptotic value. The visual observations reveal that at a small volume, bubbles are of spheroidal shape. With increase in volume, they gradually enlarge to form spherical cap bubbles and a large amount of the lighter liquid produces Taylor bubbles. Once Taylor bubbles are formed, the rise velocity remains constant.

To understand the effect of fluid properties on the rise velocity, the variation in the Froude number (Fr) with the Eötvös number (Eo) is plotted in Fig. 4. For all the liquid pairs, Fr increases sharply with Eo until it gradually reaches an asymptotic value. However, the different curves for different liquid pairs indicate the importance of fluid properties other than those included in Eo. It is interesting to note that White and Beardmore [15] performed experiments on gas-liquid systems using a wide variety of liquids and obtained a trend similar to that observed for the different liquid pairs in Fig. 4. This indicates a striking similarity between the rise of Taylor bubbles in both gas-liquid and liquid-liquid systems.

With this consideration, a simple model has been proposed to predict the shape and velocity of a LTB rising through a heavier liquid.

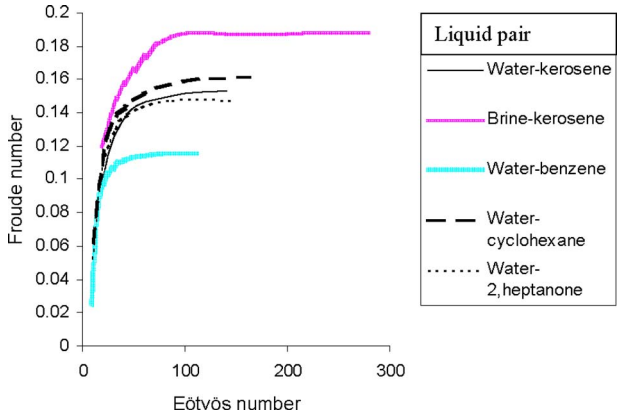

Fig. 4 Experimental Froude number as a function of the Eötvös number for the different pairs of liquids studied

4 Prediction of the Shape of LTB

A close observation of the photographs has revealed that the nose of the bubble once formed does not change with length. It is independent of bubble size and is a function of tube dimensions only. This is in agreement with the observations made for gas bubbles through stationary liquid columns. On this basis, the shape of the Taylor bubble is obtained from a potential flow analysis of the situation. The underlying assumptions of the model are as follows.

(1) Both the fluids are incompressible.
(2) The effect of viscosity is negligible.
(3) Flow is unidirectional.
(4) The origin of the frame of reference lies at the tip of the bubble nose and rises with the bubble at its rise velocity. Accordingly, the bubble appears stationary with respect to the reference frame and the primary liquid flows toward the bubble at its rise velocity (U), as shown in Fig. 5.

Following the methodology of Batchelor [8], the mass balance of the heavier liquid between AA at infinite distance from the bubble and BB at the intersection of the nose and tail region (Fig. 5) yields

$$\pi U R^2 = \pi(U + U_F)(R^2 - R_c^2) \tag{1}$$

where R is the tube radius, R_c is the equilibrium radius at the tail of the Taylor bubble (Fig. 5), U is the bubble rise velocity in the stationary liquid, and U_F is the terminal film velocity relative to the tube wall at section BB.

Rearranging Eq. (1) we get

$$U R_c^2 = U_F(R^2 - R_c^2) \tag{2}$$

Following the methodology of Dumitrescu [6], the plug flow has been assumed in the film. The asymptotic film profile in the nose region can thus be approximated as

$$R^2 U = \{R^2 - (R - \delta)^2\} U_i \tag{3}$$

where U_i, the tangential velocity at the interface, is $U+U_F$, δ, the film thickness, is $(R-r_i)$, and r_i is the radial coordinate of the interface.

For the flow of the primary liquid along the bubble surface between point 0 (stagnation point) and point 1 in Fig. 5, we apply Bernoulli's equation and obtain

$$P_0 + h_1 \rho_p g = P_1 + \tfrac{1}{2}\rho_p U_i^2 + h_2 \rho_p g \tag{4}$$

where ρ_p is the density of the primary liquid, P_0 is the pressure at point 0, the tip of the bubble nose, and P_1 is the pressure at point 1. h_1 and h_2, as denoted in Fig. 5, are the respective distances of points 0 and 1 from a reference plane.

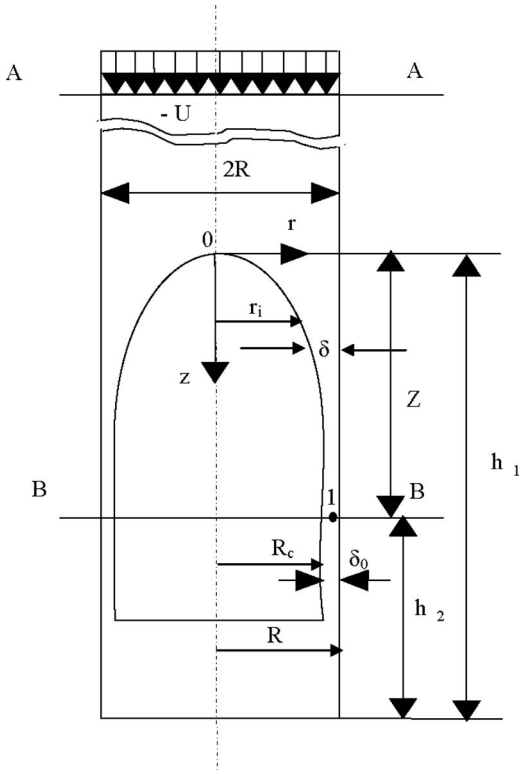

Fig. 5 Coordinate axis to predict the shape of the liquid Taylor bubble

From assumption (4), the bubble is assumed stationary with respect to the frame of reference. This gives the pressure difference $(P_1 - P_0)$ as

$$P_1 = P_0 + Z\rho_s g \tag{5}$$

where ρ_s is the density of the secondary liquid and Z, the axial distance from the bubble tip, is $(h_1 - h_2)$.

From Eqs. (4) and (5) one gets

$$P_0 + (h_1 - h_2)\rho_p g = P_0 + Z\rho_s g + \tfrac{1}{2}\rho_p U_i^2 \tag{6}$$

or

$$U_i = \left[2Zg\frac{(\rho_p - \rho_s)}{\rho_p} \right]^{1/2} \tag{7}$$

Combining Eqs. (3) and (7) we get

$$U = \left\{ 1 - \left(1 - \frac{\delta}{R} \right)^2 \right\} \left[2gZ\left(\frac{\rho_p - \rho_s}{\rho_p} \right) \right]^{1/2} \tag{8}$$

Substituting the dimensionless bubble radius as $r^* = (1 - (\delta/R))$ in Eq. (8), the final expression becomes

$$r^* = \left[1 - \mathrm{Fr}\left(\frac{R}{Z} \right)^{1/2} \right]^{1/2} \tag{9}$$

where

$$\mathrm{Fr} = \frac{U\sqrt{\rho_p}}{\sqrt{\Delta\rho g D}}$$

$\Delta\rho = \rho_p - \rho_s$ and D is the tube diameter.

The above expression shows that the bubble shape is a function of the Froude number (Fr) and the tube dimension. It does not depend on the bubble dimension, as has also been noted from photographs. The bubble shape can thus be predicted from Eq. (9) for different tube diameters and liquid pairs.

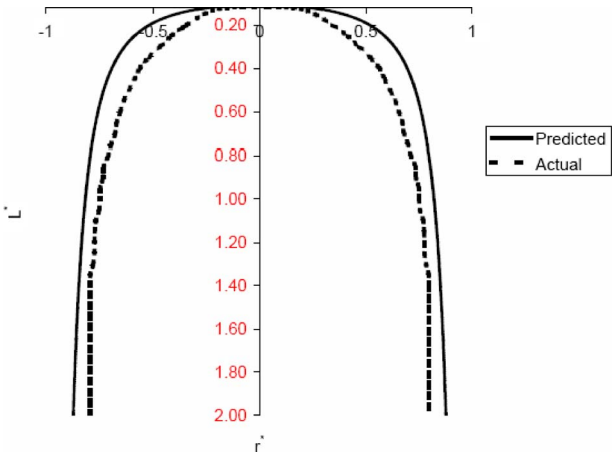

Fig. 6 Comparison between the prediction of Eq. (9) and the experimental shape of a kerosene bubble rising in a 0.0461 m i.d. tube filled with water

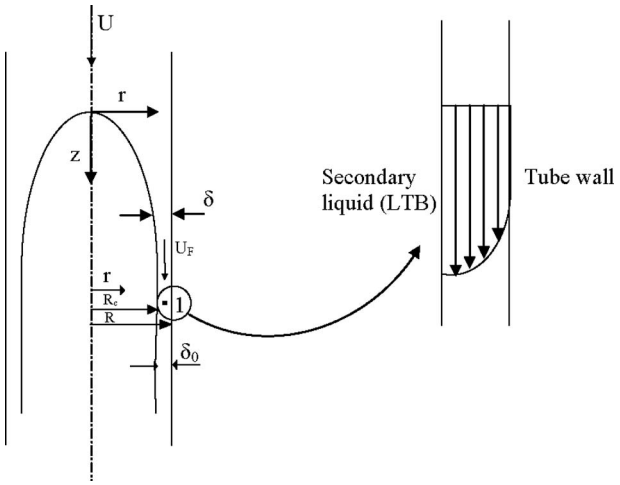

Fig. 7 The flow of primary liquid around the liquid Taylor bubble

The actual shape of the LTB has also been obtained from photographs with the help of the software IMAGE PRO-PLUS Version 5.1. A comparison between the shapes estimated from experiments and analysis is made by superimposing the two on a plot of dimensionless bubble length ($L^*=Z/R$) against the dimensionless bubble radius (r^*). One representative case for the kerosene-water pair in a 0.0461 m i.d. tube is presented in Fig. 6. The slight mismatch in the figure can be attributed to the simplifying assumptions of the model, which does not account for the effect of viscosity and surface tension.

5 Prediction of the Rise Velocity of LTB

The rise velocity is predicted from a modified form of the potential flow analysis. The model modifies the analysis by Brown [33] and incorporates the density correction as well as the effect of viscosity in the tail region of the Taylor bubble while considering the inviscid flow at the nose due to the flat velocity profile in the approach field. The assumptions underlying the model include viscous potential flow, laminar flow in the film, zero interfacial shear stress, and negligible pressure gradient along the film. With these considerations, the liquid flow in the film and nose regions has been considered in more detail with a view to obtain the rise velocity of the bubble.

6 The Film Region

Following the methodology of Brown [33] the film region has been divided into two distinct sections; one in which a portion of the liquid is accelerating freely, and the remaining portion is supported by wall shear and another in which the entire film is in steady laminar flow and supported by wall shear. The analysis of the flow in the transition region is more complex as compared with the analysis of the equilibrium laminar film.

The flow of the liquid in the equilibrium annular film of a LTB is shown in Fig. 7. The force balance on an element of the film (say at point 1) for a vertical tube gives

$$\frac{1}{r}\frac{\partial(\tau r)}{\partial r} - \rho_p g + \frac{\partial P}{\partial Z} = 0 \tag{10}$$

Now considering that $\partial P/\partial Z$ arises due to static pressure difference inside the bubble,

$$\frac{\partial P}{\partial Z} = \rho_s g$$

$$\left[\because \Delta P = Z\rho_s g, \frac{\partial P}{\partial Z} = \rho_s g\right] \tag{11}$$

Therefore Eq. (10) becomes

$$\frac{1}{r}\frac{\partial(\tau r)}{\partial r} - (\rho_p - \rho_s)g = 0 \tag{12}$$

or

$$d(\tau r) = (\rho_p - \rho_s)g r dr \tag{13}$$

where r is the radial position and τ is the shear stress.

Integrating Eq. (13) from the bubble interface to any point in the film region gives

$$\tau r = (\rho_p - \rho_s)g\frac{r^2 - R_c^2}{2} \tag{14}$$

where R_c is the equilibrium radius at the tail of the Taylor bubble.

If the primary liquid is Newtonian, then

$$\tau = \mu_p \frac{du}{dr} \tag{15}$$

where μ_p is the viscosity of the primary liquid, u is the axial component of velocity, and r is the radial position.

Substituting Eq. (15) in Eq. (14) we get

$$du = (\rho_p - \rho_s)g\frac{r^2 - R_c^2}{2\mu_p r}dr \tag{16}$$

The velocity distribution in the film is obtained by integrating Eq. (16) from r (any radial position) to R (tube radius) as follows:

$$-u = \left(\frac{\rho_p - \rho_s}{2\mu_p}\right)g\left[\frac{R^2 - r^2}{2} - R_c^2 \ln\frac{R}{r}\right] \tag{17}$$

This gives the average velocity of the liquid in the film from a balance of the volumetric flow rates as

$$\pi U_F(R^2 - R_c^2) = 2\pi\int_{R_c}^{R} u r dr \tag{18}$$

Combining Eqs. (17) and (18) we get

$$U_F = \frac{\rho_p - \rho_s}{\mu_p} g \left[\frac{R_c^4}{2(R^2 - R_c^2)} \ln \frac{R_c}{R} + \frac{3R_c^2}{8} - \frac{R^2}{8} \right] \tag{19}$$

From Eqs. (2) and (19) we get

$$U = \frac{\rho_p - \rho_s}{\mu_p} g \frac{R^2}{\left(1 - \frac{\delta}{R}\right)^2} \left[\frac{2}{3} \left(\frac{\delta}{R}\right)^3 \left(1 - \frac{\delta}{R}\right) + \frac{1}{10} \left(\frac{\delta}{R}\right)^5 + \frac{1}{60} \left(\frac{\delta}{R}\right)^6 + \cdots \right] \tag{20}$$

The above equation can be expressed in terms of relative film thickness $\xi_0(\delta_0/R)$ as

$$U = \frac{\rho_p - \rho_s}{\mu_p} g \frac{R^2}{(1 - \xi_0)^2} \left[\frac{2}{3} \xi_0^3 (1 - \xi_0) + \frac{1}{10} \xi_0^5 + \frac{1}{60} \xi_0^6 + \cdots \right] \tag{21}$$

where δ_0 is the terminal film thickness in the tail region of the LTB beyond line BB in Fig. 5 and R is the tube radius.

Neglecting the higher order term greater than 4, the equation reduces to

$$U = \frac{2}{3} \frac{\rho_p - \rho_s}{\mu_p} g R^2 \frac{\xi_0^3}{1 - \xi_0} \tag{22}$$

7 Nose Region

From the potential flow analysis at the nose region, as mentioned by Brown [33], the velocity of the Taylor bubbles are well correlated by the equation

$$U = 0.496 \sqrt{g R_c} \tag{23}$$

Upon introducing the density correction term the above equation becomes

$$U = 0.496 \sqrt{\frac{\rho_p - \rho_s}{\rho_p} g R_c} \tag{24}$$

A simultaneous solution of Eqs. (22) and (24) gives the equilibrium film thickness as

$$\delta_0 = \frac{-1 + \sqrt{1 + 4NR}}{2N} \tag{25}$$

where

$$N = \left[1.81 \frac{(\rho_p - \rho_s)\rho_p}{\mu_p^2} g \right]^{1/3} \tag{26}$$

Expressing R_c in terms of N,

$$R_c = R - \delta_0 = R \left(1 - \frac{-1 + \sqrt{1 + 4NR}}{2NR} \right) \tag{27}$$

and combining Eqs. (24) and (27), we get

$$U = 0.496 \sqrt{\frac{\rho_p - \rho_s}{\rho_p} g R} \sqrt{1 - \frac{-1 + \sqrt{1 + 4NR}}{2NR}} \tag{28}$$

Equation (28) can be used to predict the rise velocity of a Taylor bubble by accounting for the density and viscosity effects. An attempt has next been made to incorporate the effect of surface tension in the expression.

A survey of the past literature shows that in gas-liquid systems the different correlations for the rise of TBs generally account for the influence of surface tension by using the Eötvös number $[g(\rho_p - \rho_s)D^2/\sigma]$. Different researchers [29,38,40] proposed different expressions including Eo in their correlations. For large buoyancy Reynolds number ($\mathrm{Re}_b > 200$), Wallis [40] considered the effect of interfacial tension using the following function of the Eötvös number:

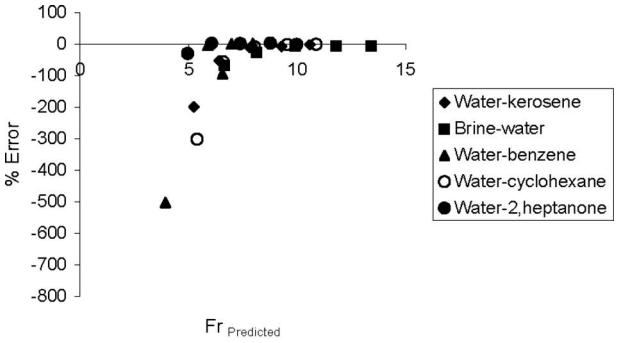

(*a*) % Error in prediction of Eq. (28)

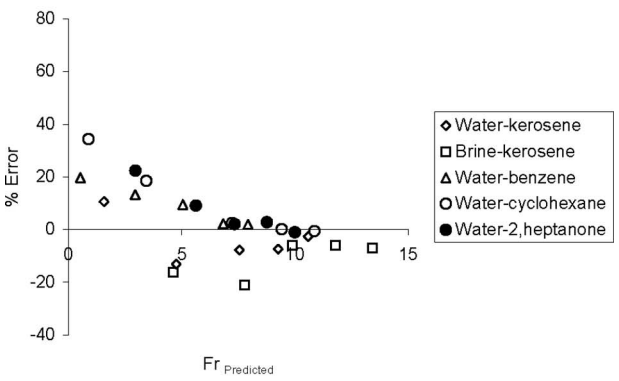

(*b*) % Error in prediction of Eq. (29)

Fig. 8 Percentage error in prediction of rise velocity of a liquid Taylor bubble

$$\frac{1}{\left(1 + \frac{3805}{\mathrm{Eo}^{3.06}}\right)^{0.58}}$$

Incorporating the same factor in Eq. (28), the final expression of the rise velocity is obtained as

$$U = 0.496 \sqrt{\frac{\rho_p - \rho_s}{\rho_p} g R} \sqrt{1 - \frac{-1 + \sqrt{1 + 4NR}}{2NR}} \frac{1}{\left(1 + \frac{3805}{\mathrm{Eo}^{3.06}}\right)^{0.58}} \tag{29}$$

The above analysis yields a semi-empirical equation, which accounts for the effects of surface tension, viscous effects, and density difference between the two liquids. The predictions of the equation have been validated with the experimental results for different tube diameters and liquid properties. These validations are presented in Fig. 8 and Table 2. In Fig. 8 the percentage error is plotted against the predicted Froude number where the percentage error is calculated based on the experimental value. The figure shows the improvement in prediction of Eq. (29) as compared with Eq. (28). Moreover predictions are better for some liquid pairs, namely, water-kerosene, brine-kerosene, and water-benzene.

The results are also listed in Table 2 along with the buoyancy Reynolds number ($\mathrm{Re}_b = [D^3 g(\rho_p - \rho_s)\rho_p]^{1/2}/\mu_p$) for each case to show the diameter effect on the predicted results. The table shows that the theoretical values are close to the experimental results for pipes of larger diameters while the deviation is consistently higher for tubes of 0.012 m and 0.0176 m diameter. It is felt that this discrepancy arises because the present analysis does not consider the effect of the viscosity of the secondary liquid. This may be justifiable in the analysis of rising gas bubbles, as the viscosity of

Table 2 Comparison of predicted results with experimental results

Sl. No.	Liq. Pair	$D\times10^2$ (m)	$\mathrm{Re}_b\times10^{-3}$	$U_{expt}\times10^2$ (m/s)	$U_{predicted}$ from Eq. (28) $\times10^2$ (m/s)	Deviation (%)	$U_{predicted}$ from Eq. (29)$\times10^2$ (m/s)	Deviation (%)
1	Kerosene bubble in water	1.2	1.90	1.75	5.24	−199.6	1.56	10.6
		1.76	3.38	4.21	6.42	−52.61	4.76	−13.1
		2.57	5.96	6.99	7.82	−11.9	7.54	−7.8
		3.58	9.79	8.6	9.29	−7.93	9.25	−7.4
		4.61	14.31	10.3	10.6	−2.73	10.58	−2.6
2	Kerosene bubble in brine	1.2	2.90	3.96	6.4	−67.7	4.61	−16.36
		1.76	5.15	6.4	8.1	−26.9	7.76	−21.12
		2.57	9.08	9.3	9.9	−6.45	9.88	−5.95
		3.58	14.94	11.1	11.8	−6.2	11.78	−6.13
		4.61	21.82	12.55	13.4	−7.06	13.43	−7.05
3	Benzene bubble in water	1.2	1.43	0.65	3.93	−502.8	0.52	19.7
		1.76	2.54	3.39	6.56	−93.8	2.94	13.3
		2.57	4.49	5.58	5.87	−5.2	5.05	9.5
		3.58	7.38	6.98	6.98	0.023	6.83	2.2
		4.61	10.78	8.08	7.96	1.5	7.92	1.97
4	Cyclohexane bubble in water	1.2	1.95	1.3	5.4	−302.3	0.88	34.3
		1.76	3.47	4.2	6.6	−56.8	3.43	18.5
		2.57	6.12	7.4	8.04	−8.69	7.22	2.5
		3.58	10.06	9.4	9.55	−1.42	9.4	0.14
		4.61	14.71	10.8	10.88	−0.96	10.85	−0.62
5	2,heptanone bubble in water	1.2	1.79	3.81	4.95	−29.97	2.95	22.4
		1.76	3.18	6.18	6.06	2.03	5.62	9.1
		2.57	5.61	7.48	7.38	1.3	7.3	2.07
		3.58	9.22	9.01	8.77	2.65	8.76	2.75
		4.61	13.48	9.89	9.99	−1.07	9.99	−1.05

gas is substantially lower than the viscosity of the surrounding liquid. On the contrary, the viscosities of the primary and secondary fluids are of comparable orders of magnitude in the present case.

8 Conclusions

Based on potential flow theory, a model has been proposed to predict the shape of a liquid Taylor bubble. The slight deviations between the predicted and actual shapes suggest the limitations of the theory. Accordingly, it has been modified to predict the rise velocity of the LTBs. The modified analysis incorporates the effect of viscosity of the primary fluid, density difference between the two liquids, and surface tension effects. The analysis by Brown [33] has been considered for this purpose and the laminar film solution at the tail region is coupled with the potential flow theory at the nose region. The effect of surface tension has been considered from the correlation proposed by Wallis [40]. The predictions of the analysis are in close agreement with experimental data on rise velocity for most of the cases. The only exceptions are at small pipe diameters. This probably arises due to the limitations of the semi-empirical approach.

The complex hydrodynamics of a liquid Taylor bubble can be explained from a rigorous analysis starting from the basic physics of the flow situation. Computational techniques may be adopted for this purpose. Extensive experiments are required to study the effect of viscosity of the secondary fluid on the rise velocity of the Taylor bubble and to incorporate this effect in the theoretical analysis.

Nomenclature

Eo = Eötvös number$=(\rho_p-\rho_s)gD^2/\sigma$

Fr = Froude number$=U\sqrt{\rho_p}/\sqrt{\Delta\rho gD}$

Re_b = buoyancy Reynolds number$=[D^3g(\rho_p-\rho_s)\rho_p]^{1/2}/\mu_p$

h_1, h_2 = respective distances of points 0 and 1 from a reference plane in Fig. 5 (m)

L^* = dimensionless bubble length$=Z/R$

r^* = dimensionless bubble radius$=(1-\delta/R)$

D = tube diameter (m)

N = dimensional parameter (m^{-1})

P_0 = pressure at the tip of the bubble nose (Pa)

P_1 = pressure at point 1 (Pa)

R = tube radius (m)

R_c = equilibrium radius at the tail of the Taylor bubble (m)

U = bubble rise velocity in stationary liquid (m/s)

U_F = average liquid velocity in the film relative to the tube wall (m/s)

U_i = tangential velocity at the interface (m/s)

g = gravitational acceleration (m/s^2)

r = radial position (m)

r_i = radial coordinate of the interface

u = axial component of velocity (m/s)

Z = axial distance from the bubble tip (m)

Greek Letters

δ = film thickness at any radial position as shown in Fig. 5 $=R-r_i$ (m)

δ_0 = terminal film thickness in tail region as shown in Fig. 5 $=R-R_c$ (m)

ρ_p = density of the primary liquid (kg/m^3)

ρ_s = density of the secondary liquid (kg/m^3)

$\Delta\rho$ = $(\rho_p-\rho_s)$ (kg/m^3)

τ = shear stress (N/m^2)

ξ_0 = dimensionless terminal film thickness$=\delta_0/R$

μ_p = viscosity of primary liquid (mPa s)
σ = interfacial tension (N/m)

References

[1] Zukoski, E. E., 1966, "Influence of Viscosity, Surface Tension, and Inclination Angle on Motion of Long Bubbles in Closed Tubes," J. Fluid Mech., **25**, pp. 821–837.

[2] Couet, B., and Strumolo, G. S., 1987, "The Effects of Surface Tension and Tube Inclination on a Two-Dimensional Rising Bubble," J. Fluid Mech., **184**, pp. 1–14.

[3] Fagundes Netto, J. R., Fabre, J., and Peresson, L., 1999, "Shape of Long Bubbles in Horizontal Slug Flow," Int. J. Multiphase Flow, **25**, pp. 1129–1160.

[4] Bi, C. Q., and Zhao, T. S., 2001, "Taylor Bubbles in Miniaturized Circular and Noncircular Channels," Int. J. Multiphase Flow, **27**, pp. 561–570.

[5] Wallis, G. B., 1969, *One-Dimensional Two-Phase Flow*, McGraw-Hill, New York.

[6] Dumitrescu, D. T., 1943, "Stromung and Einer Luftbluse in Senkrechten rohr," Z. Angew. Math. Mech., **23**, pp. 139–149.

[7] Davies, R. M., and Taylor, G., 1950, "The Mechanics of Large Bubbles Rising Through Extended Liquids and Through Liquids in Tubes," Proc. R. Soc. London, Ser. A, **200**, pp. 375–390.

[8] Batchelor, G. K., 1967, *An Introduction to Fluid Dynamics*, Cambridge University, Cambridge, England.

[9] Collins, R., De Moraes, F. F., Davidson, J. F., and Harrison, D., 1978, "The Motion of the Large Gas Bubble Rising Through Liquid Flowing in a Tube," J. Fluid Mech., **89**, pp. 497–514.

[10] Bendiksen, K. H., 1985, "On the Motion of Long Bubbles in Vertical Tubes," Int. J. Multiphase Flow, **11**, pp. 797–812.

[11] Batchelor, G. K., 1987, "The Stability of a Large Gas Bubble Rising Through Liquid," J. Fluid Mech., **184**, pp. 399–442.

[12] Reinelt, D. A., 1987, "The Rate at Which a Long Bubble Rises in Vertical Tube," J. Fluid Mech., **175**, pp. 557–565.

[13] Funada, T., Joseph, D. D., Maehara, T., and Yamashita, S., 2005, "Ellipsoidal Model of the Rise of a Taylor Bubble in a Round Tube," Int. J. Multiphase Flow, **31**, pp. 473–491.

[14] Harmathy, T. Z., 1960, "Velocity of Large Drops and Bubbles in Media of Infinite or Restricted Extent," AIChE J., **6**, pp. 281–288.

[15] White, E. T., and Beardmore, R. H., 1962, "The Velocity of Rise of Single Cylindrical Air Bubbles Through Liquids Contained in Vertical Tubes," Chem. Eng. Sci., **17**, pp. 351–361.

[16] Maneri, C. C., and Zuber, N., 1974, "An Experimental Study of Plane Bubbles Rising Inclination," Int. J. Multiphase Flow, **1**, pp. 623–645.

[17] Bhaga, T., and Weber, M., 1981, "Bubbles in Viscous Liquids: Shapes, Wakes and Velocities," J. Fluid Mech., **105**, pp. 61–85.

[18] Nigmatulin, T. R., and Bonetto, F. J., 1997, "Shape of Taylor Bubbles in Vertical Tubes," Int. Commun. Heat Mass Transfer, **24**, pp. 1177–1185.

[19] Salman, W., Gavriilidis, A., and Angeli, P., 2006, "On the Formation of Taylor Bubbles in Small Tubes," Chem. Eng. Sci., **61**, pp. 6653–6666.

[20] Nogueira, S., Riethmuler, M. L., Campos, J. B. L. M., and Pinto, A. M. F. R., 2006, "Flow in the Nose Region and Annular Film Around a Taylor Bubble Rising Through Vertical Columns of Stagnant and Flowing Newtonian Liquids," Chem. Eng. Sci., **61**, pp. 845–857.

[21] Birkhoff, G., and Carter, D., 1957, "Rising Plane Bubbles," J. Math. Mech., **6**, pp. 769–779.

[22] Miksis, M. J., Vanden-Broeck, J.-M., and Keller, J. B., 1982, "Rising Bubbles," J. Fluid Mech., **123**, pp. 31–41.

[23] Mao, Z., and Dukler, A. E., 1990, "The Motion of Taylor Bubbles in Vertical Tubes. I. A Numerical Simulation for the Shape and Rise Velocity of Taylor Bubbles in Stagnant and Flowing Liquids," J. Comput. Phys., **91**, pp. 132–160.

[24] Bugg, J. D., Mack, K., and Rezkallah, K. S., 1998, "A Numerical Model of Taylor Bubbles Rising Through Stagnant Liquids in Vertical Tubes," Int. J. Multiphase Flow, **24**, pp. 271–281.

[25] Daripa, P., 2000, "A Computational Study of Rising Plane Taylor Bubbles," J. Comput. Phys., **157**, pp. 120–142.

[26] Bretherton, F. P., 1961, "The Motion of Long Bubbles in Tubes," J. Fluid Mech., **10**, pp. 166–188.

[27] Tung, K. W., and Parlange, J. Y., 1976, "Note on the Motion of Long Bubbles in Closed Tubes-Influence of Surface Tension," Acta Mech., **24**, pp. 313–317.

[28] Vanden-Broeck, J.-M., 1984, "Rising Bubbles in a Two-Dimensional Tube With Surface Tension," Phys. Fluids, **27**, pp. 2604–2607.

[29] Nickens, H. V., and Yannitell, D. W., 1987, "The Effects of Surface Tension and Viscosity on the Rise Velocity of a Large Gas Bubble in a Closed Vertical Liquid-Liquid Tube," Int. J. Multiphase Flow, **13**, pp. 57–69.

[30] Couet, B., Strumolo, G. S., and Dukler, A. E., 1986, "Modeling of Two-Dimensional Bubbles in a Rectangular Channel of Finite Width," Phys. Fluids, **29**, pp. 2367–2372.

[31] Garabedian, P. R., 1957, "On Steady-State Bubbles Generated by Taylor Instability," Proc. R. Soc. London, Ser. A, **241**, pp. 423–431.

[32] Goldsmith, H. L., and Mason, S. G., 1962, "The Motion of Single Large Bubbles in Closed Vertical Tubes," J. Fluid Mech., **14**, pp. 42–58.

[33] Brown, R. A. S., 1965, "The Mechanics of Large Gas Bubbles in Tubes. I. Bubble Velocities in Stagnant Liquids," Can. J. Chem. Eng., **Q2**, pp. 217–223.

[34] Pinto, A. M. F. R., and Campos, J. B. L. M., 1996, "Coalescence of Two Gas Slugs Rising in a Vertical Column of Liquid Pinto and Campos," Chem. Eng. Sci., **51**, pp. 45–54.

[35] Nogueira, S., Riethmuler, M. L., Campos, J. B. L. M., and Pinto, A. M. F. R., 2006, "Flow in the Nose Region and Annular Film Around a Taylor Bubble Rising Through Vertical Columns of Stagnant and Flowing Newtonian Liquids," Chem. Eng. Sci., **61**, pp. 845–857.

[36] Nogueira, S., Riethmuler, M. L., Campos, J. B. L. M., and Pinto, A. M. F. R., 2006, "Flow Patterns in the Wake of a Taylor Bubble Rising Through Vertical Columns of Stagnant and Flowing Newtonian Liquids: An Experimental Study," Chem. Eng. Sci., **61**, pp. 7199–7212.

[37] Liao, Q., and Zhao, T. S., 2003, "Modeling of Taylor Bubble Rising in a Vertical Mini Noncircular Channel Filled With a Stagnant Liquid," Int. J. Multiphase Flow, **29**, pp. 411–434.

[38] Clanet, C., Heraud, P., and Searby, G., 2004, "On the Motion of Bubbles in Vertical Tubes of Arbitrary Cross-Sections: Some Complements to the Dumitrescu–Taylor Problem," J. Fluid Mech., **519**, pp. 359–376.

[39] Clift, R., Grace, J. R., and Weber, M. E., 1978, *Bubbles, Drops, and Particles*, Academic, New York.

[40] Wallis, G. B., 1962, "General Correlations for the Rise Velocity of Cylindrical Bubbles in Vertical Tubes," General Engineering Laboratory, General Electric Co., Report No. 62GL130.

[41] Tomiyama, A., Nakahara, Y., Adachi, Y., and Hosokawa, S., 2003, "Shapes and Rising Velocities of Single Bubbles Rising Through an Inner Subchannel," J. Nucl. Sci. Technol., **40**, pp. 136–142.

[42] Viana, F., Pardo, R., Yanez, R., Trallero, J. L., and Joseph, D. D., 2003, "Universal Correlation for the Rise Velocity of Long Bubbles in Round Pipes," J. Fluid Mech., **494**, pp. 379–398.

[43] Brauner, N., and Ullmann, A., 2004, "Modeling of Gas Entrainment From Taylor Bubbles: Part A: Slug Flow," Int. J. Multiphase Flow, **30**, pp. 239–272.

[44] Brauner, N., and Ullmann, A., 2004, "Modeling of Gas Entrainment From Taylor Bubbles: Part B: A Stationary Bubble," Int. J. Multiphase Flow, **30**, pp. 273–290.

[45] Jana, A. K., Das, G., and Das, P. K., 2006, "A Novel Technique to Identify Flow Patterns During Liquid-Liquid Two-Phase Upflow Through a Vertical Pipe," Ind. Eng. Chem. Res., **45**, pp. 2381–2393.